Representations in density dependent hadronic field theory and compatibility with QCD sum rules

R. Aguirre

Departamento de Física, Facultad de Ciencias Exactas,
Universidad Nacional de La Plata. C. C. 67 (1900) La Plata, Republica Argentina
(Received 1 September 2005; published 31 January 2006)

Different representations of an effective, covariant theory of the hadronic interaction are examined. For this purpose we have introduced nucleon-meson vertices parametrized in terms of scalar combinations of hadronic fields, extending the conceptual frame of the density-dependent hadronic field theory. Nuclear matter properties at zero temperature are examined in the mean-field approximation, including the equation of state, the Landau parameters, and collective modes. The treatment of isospin channels, which includes quantum chromodynamics sum-rules inputs, is outlined.

I. INTRODUCTION

In present-day theoretical physics a generalized concept is that the description of all physical phenomena should be derivable from first principles in a unified way. However, the bridge toward concrete applications requires elaborated procedures and judicious arguments. This is the case of quantum chromodynamics (QCD), which is the accepted theoretical model for strong interactions. Despite the fact that it is perturbative in the high-energy realm, the fundamental state of matter corresponds to the opposite limit, where confinement and breakdown of symmetries make it mathematically intractable. Different effective models, such as Nambu–Jona-Lasinio, Skyrme, baglike, and chiral perturbation theory attempt to translate the main features of QCD into the hadronic phase. Lattice simulations and QCD sum rules are techniques which share this aim but use different methods.

The QCD sum rules are an ingenious procedure to reveal the foundations of certain hadronic properties. The method is based on the evaluation of correlation functions in terms of quark and gluon degrees. They are expressed as combinations of perturbative contributions and condensates (nonperturbative) by using operator product expansion. Finally, this expansion is connected with the hadronic counterpart by means of a Borel transformation. The method was developed to study meson [1] as well as baryon [2] properties in a vacuum; afterward it was generalized to study finite-density systems [3,4]. These calculations provide a useful guide for some static properties of hadrons immersed in a dense medium, with respect to QCD symmetries and phenomenology. However, the method is not able to take into account the dynamical aspects of hadronic matter, which may be achieved by inserting these results coherently into a theoretical model of hadronic interactions.

A similar situation was found in nuclear structure studies, which yield reliable density-dependent nucleon self-energies by combining *microscopic* potentials and the relativistic Dirac-Brueckner approximation for nuclear matter. Notwithstanding, this procedure was inadequate to treat finite nuclei because of unsurmountable mathematical difficulties. A feasible solution to this dilemma was proposed in Refs. [5–8], where

density-dependent vertices are defined in terms of the self-energies obtained in Dirac-Brueckner calculations. The enlarged hadronic field model keeps the mathematical versatility of the quantum hadrodynamic models [9] but is equipped with couplings reflecting the properties of the nuclear environment. The structure of spherical nuclei, in the medium to heavy range, was studied within this framework using the Hartree approximation.

Further improvements, developed in Ref. [7], replace the density dependence of the meson-nucleon vertices by an expansion in terms of in-medium nucleon condensates. This conceptual replacement restores the covariance and the thermodynamical consistency of the model, giving rise to the density-dependent hadronic field theory (DDHFT). It has been recently appended by introducing momentum-dependent vertices [10] and an expansion of the vertices in terms of meson mean-field values [11].

The validity of the method is justified only *a posteriori* and relies on the flexibility of hadronic field models to accommodate pieces of information provided by another field of research. The enlarged model yields a simpler and more intuitive description, instead of making involved calculations based on first-principles interactions. A significant exemplification of this standpoint was given by the Brown-Rho scaling of hadronic masses. Taking into account the chiral and scale symmetries of QCD solely, an approximate scaling law for the in-medium hadronic masses was derived in Ref. [12]. This hypothesis was applied to describe heavy-ion collisions, reaching an excellent agreement with the experimental results for the low-mass dilepton production rate [13].

Given a set of physically meaningful self-energies as input for DDHFT, there is room for a full family of hadronic models, according to the field parametrization of the vertices. This ambiguity may lead to different predictions for nuclear observables. This point has not been investigated yet, and it is the main purpose of the present work.

Previously the author attempted to apply the scheme outlined above to relate nuclear observables with QCD inspired results. For this purpose the nucleon self-energies obtained in Ref. [4] by using QCD sum rules were used as input. However, Ref. [11] does not exhaust the physical description given

there, as it covers also isospin asymmetric nuclear matter. Consequently, we aim to complete our theoretical model, including isospin degrees of freedom, based on the results presented in Ref. [4].

In the next section we present the general features of DDHFT, specifically the meson parametrization of the hadronic vertices. In Sec. III the results for symmetric nuclear matter are presented and discussed. Finally, Sec. IV is devoted to the summary and conclusions.

II. DENSITY-DEPENDENT HADRONIC FIELD THEORY

As mentioned above, DDHFT was designed to incorporate pieces of information produced by other theoretical frames into the hadronic field formalism. Strictly speaking, DDHFT takes as input the nucleon self-energies, which can be decomposed into isoscalar and isovector components. Each one contains Lorentz scalar and vector contributions: i.e., Σ_s^{in}, Σ_μ^{in}, $\Sigma_s^{in\,a}$, $\Sigma_\mu^{in\,a}$, where the superscript a distinguishes isovector quantities and $a = 1, 2$ stands for proton and neutron, respectively. For homogeneous nuclear matter in steady state, they can be parametrized as functions of continuous parameters, such as baryonic current density j_μ and temperature, characterizing the macroscopic state of hadronic matter. In particular, there exists a reference frame where the mean value of the spatial part of the baryonic current vanishes. In its original version Σ^{in} was taken from relativistic Brueckner-Hartree-Fock calculations with one-boson exchange potentials [5].

In addition, a Lagrangian density is proposed in terms of meson fields σ, ω_μ in the isoscalar sector and ϕ_c, ρ_μ^c in the isovector one. The indices $c = 1, 2, 3$ stand for the meson isospin projection

$$
\begin{aligned}
\mathcal{L} &= \bar{\Psi}\big(i\,\slashed{\partial} - M + \Gamma_s\,\sigma - \Gamma_w\,\slashed{\phi} + \Gamma_f^c\,\phi_c + \Gamma_r^c\,\slashed{\rho}_c\big)\Psi \\
&\quad + \tfrac{1}{2}\big(\partial_\mu\sigma\,\partial^\mu\sigma - m_s^2\sigma^2\big) - \tfrac{1}{4}W_{\mu\nu}W^{\mu\nu} + \tfrac{1}{2}m_w^2\omega_\mu\omega^\mu \\
&\quad + \tfrac{1}{2}\big(\partial_\mu\phi_c\partial^\mu\phi_c - m_f^2\phi^2\big) - \tfrac{1}{4}R_{\mu\nu}^c R_c^{\mu\nu} + \tfrac{1}{2}m_r^2\rho_\mu^c\rho_c^\mu, \quad (1)
\end{aligned}
$$

where $W_{\mu\nu} = \partial_\mu\omega_\nu - \partial_\nu\omega_\mu$ and $R_{\mu\nu}^c = \partial_\mu\rho_\nu^c - \partial_\nu\rho_\mu^c$ have been used and Ψ represents an isospinor. We have adopted the convention that repeated isospin indices must be summed. The isovector vertices Γ^c take values over the space generated by the Pauli matrices τ and the identity. The masses have been fixed at the phenomenological values $M = 940$ MeV, $m_w = 783$ MeV, $m_s = 550$ MeV, $m_r = 770$ MeV, and $m_f = 984$ MeV. The isoscalar vertices are assumed to depend on the scalar combinations: $s_1 = \sqrt{j_\mu j^\mu}$, $s_2 = \bar{\Psi}\Psi$, $m_1 = \sqrt{\omega_\mu\omega^\mu}$, and $m_2 = \sigma$, whereas the isovector Γ^c could depend linearly on $j_c = \bar{\Psi}\tau^c\Psi$, or ϕ_c, and on the scalars $s_3 = \sqrt{j_\mu^c j_c^\mu}$, $s_4 = \sqrt{j_c j_c}$, $m_3 = \sqrt{\rho_\mu^c\rho_c^\mu}$, and $m_4 = \sqrt{\phi_c\phi_c}$. The baryonic and isospin current have been written as $j_\mu = \bar{\Psi}\gamma_\mu\Psi$ and $j_\mu^c = \bar{\Psi}\gamma_\mu\tau^c\Psi$, respectively. This is not the most general dependence, but it keeps a clear separation between isospin scalar and vector degrees of freedom. In Ref. [7] the dependence on s_1 or s_2 was presented and the case with only s_2 was explicitly studied. In Ref. [11] the meson dependence of the vertices was introduced within DDHFT for symmetric nuclear matter.

The field equations for this Lagrangian density are as follows:

$$
\begin{aligned}
&\big[(i\,\slashed{\partial} - M + \Gamma_s\,\sigma - \Gamma_w\,\slashed{\phi})\delta_{AB} + \Gamma_{f\,AB}^c\,\phi_c + \Gamma_{r\,AB}^c\,\slashed{\rho}_c\big]\psi_B \\
&\quad + \bar{\Psi}\frac{\partial}{\partial\bar{\psi}_A}\big(\Gamma_s\sigma - \Gamma_w\,\slashed{\phi} + \Gamma_f^c\,\phi_c + \Gamma_r^c\,\slashed{\rho}_c\big)\Psi = 0 \quad (2)
\end{aligned}
$$

$$
\big(\Box + m_s^2\big)\sigma = \bar{\Psi}\left[\Gamma_s + \left(\frac{\partial\Gamma_s}{\partial m_2}\sigma - \frac{\partial\Gamma_w}{\partial m_2}\,\slashed{\phi}\right)\right]\Psi \quad (3)
$$

$$
\partial_\mu W^{\mu\nu} + m_w^2\omega^\nu = \bar{\Psi}\left[\Gamma_w\gamma^\nu - \frac{\partial m_1}{\partial\omega_\nu}\left(\frac{\partial\Gamma_s}{\partial m_1}\sigma - \frac{\partial\Gamma_w}{\partial m_1}\,\slashed{\phi}\right)\right]\Psi \quad (4)
$$

$$
\big(\Box + m_f^2\big)\phi^c = \bar{\Psi}\left[\Gamma_f^c + \frac{\partial m_4}{\partial\phi_c}\left(\frac{\partial\Gamma_f^a}{\partial m_4}\phi_a + \frac{\partial\Gamma_r^a}{\partial m_4}\,\slashed{\rho}_a\right)\right]\Psi \quad (5)
$$

$$
\begin{aligned}
\partial_\mu R_c^{\mu\nu} + m_r^2\rho_c^\nu &= -\bar{\Psi}\left[\Gamma_{r\,c}\gamma^\nu + \frac{\partial m_3}{\partial\rho_c^\nu}\left(\frac{\partial\Gamma_f^a}{\partial m_3}\phi_a\right.\right. \\
&\quad \left.\left. + \frac{\partial\Gamma_r^a}{\partial m_3}\,\slashed{\rho}_a\right)\right]\Psi, \quad (6)
\end{aligned}
$$

where the isospin indices have been denoted as A, $B = 1, 2$ for nucleons and a, $c = 1, 2, 3$ for mesons. In the first equation, the vertex derivatives must be interpreted as

$$
\frac{\partial\Gamma}{\partial\bar{\psi}_A} = \sum_1^4 \frac{\partial\Gamma}{\partial s_k}\frac{\partial s_k}{\partial\bar{\psi}_A}.
$$

The mean-field approximation (MFA) is suited to describe homogeneous matter. Within this scheme, meson fields are replaced by their uniform mean values and bilinear combinations of spinors are replaced by their expectation values. For homogeneous, isotropic nuclear matter in steady state, some simplifications arise in the meson mean values. For instance, their spatial dependence can be neglected; only the timelike components of the vector, ω_μ and ρ_μ, and only the third component of the isovector mesons are nonzero.

As a result Eqs. (2)–(6) reduce, within MFA, to

$$
0 = \big[(i\,\slashed{\partial} - M)\,\delta_{AB} + \Sigma_s^{AB} - \slashed{\Sigma}^{AB}\big]\psi_B, \quad (7)
$$

$$
m_s^2\tilde{\sigma} = \langle\bar{\Psi}\,\Gamma_s\Psi\rangle + \left\langle\bar{\Psi}\frac{\partial\Gamma_s}{\partial m_2}\Psi\,\sigma\right\rangle - \left\langle\bar{\Psi}\frac{\partial\Gamma_w}{\partial m_2}\gamma_\mu\Psi\omega^\mu\right\rangle; \quad (8)
$$

$$
\begin{aligned}
g_0^\nu m_w^2\tilde{\omega} &= \langle\bar{\Psi}\,\Gamma_w\gamma^\nu\Psi\rangle - \left\langle\bar{\Psi}\frac{\partial\Gamma_s}{\partial m_1}\Psi\,\frac{\sigma\omega^\nu}{m_1}\right\rangle \\
&\quad + \left\langle\bar{\Psi}\frac{\partial\Gamma_w}{\partial m_1}\gamma_\mu\Psi\,\frac{\omega^\nu\omega^\mu}{m_1}\right\rangle; \quad (9)
\end{aligned}
$$

$$
\begin{aligned}
\delta_{3c}\,m_f^2\tilde{\phi} &= \langle\bar{\Psi}\Gamma_f^c\Psi\rangle + \left\langle\bar{\Psi}\frac{\partial\Gamma_f^a}{\partial m_4}\Psi\,\frac{\phi_c\phi_a}{m_4}\right\rangle \\
&\quad + \left\langle\bar{\Psi}\frac{\partial\Gamma_r^a}{\partial m_4}\gamma_\mu\Psi\,\frac{\phi_c}{m_4}\rho_a^\mu\right\rangle; \quad (10)
\end{aligned}
$$

$$
\begin{aligned}
-\delta_{3c}g_0^\nu m_r^2\tilde{\rho} &= \langle\bar{\Psi}\Gamma_{r\,c}\gamma^\nu\Psi\rangle + \left\langle\bar{\Psi}\frac{\partial\Gamma_f^a}{\partial m_3}\Psi\,\frac{\rho_c^\nu\phi_a}{m_3}\right\rangle \\
&\quad + \left\langle\bar{\Psi}\frac{\partial\Gamma_r^a}{\partial m_3}\gamma_\mu\Psi\,\frac{\rho_c^\nu\rho_a^\mu}{m_3}\right\rangle; \quad (11)
\end{aligned}
$$

here tildes over the meson symbols stand for their mean-field values, and the two last terms within brackets in Eq. (7) can be considered as the scalar and vector components of the nucleon self-energies:

$$\Sigma_s^{AB} = \langle \Gamma_s \sigma + \bar{\Psi} \Lambda_2 \Psi \rangle \delta_{AB}$$
$$+ \left\langle \Gamma_f^{c\,AB} \phi_c + \tau_a^{AB} \, \bar{\Psi} \Lambda_4 \Psi \, \frac{\bar{\Psi} \tau_a \Psi}{s_4} \right\rangle, \qquad (12)$$

$$\Sigma_v^{AB} = \left\langle \Gamma_w \omega_v - \bar{\Psi} \Lambda_1 \frac{j_v}{s_1} \Psi \right\rangle \delta_{AB}$$
$$- \left\langle \Gamma_{rc}^{AB} \rho_v^c + \tau_a^{AB} \, \bar{\Psi} \Lambda_3 \Psi \, \frac{j_v^a}{s_3} \right\rangle, \qquad (13)$$

with $\Lambda_k = \partial(\Gamma_s \sigma - \Gamma_w \phi + \Gamma_f^c \phi_c + \Gamma_r^c \, \rho_c)/\partial s_k$.

For the sake of concreteness, we have examined three possible parametrizations:

(a) symmetric nuclear matter, with $\Gamma_s(s_1)$, $\Gamma_w(s_1)$;

(b) symmetric nuclear matter, with $\Gamma_s(s_2)$, $\Gamma_w(s_1)$;

(c) asymmetric nuclear matter, with $\Gamma_s(m_2)$, $\Gamma_w(m_1)$, $\Gamma_f^c(\phi^c, m_4)$, $\Gamma_r^c = \Gamma_r(\phi^c, m_3)$.

The first two cases are comparable to the instances presented in Ref. [7] as vector and scalar dependencies. The last case is a development of the preliminaries calculations of Ref. [11], the field dependence of the isospin vertices have been chosen so as to adjust the QCD sum rules calculations in Ref. [4].

These results are simplified within the assumptions (a)–(c) above; for the sake of completeness we consider separately each of these cases:

(a)

$$\Sigma_s = \Gamma_s \tilde{\sigma}, \; \Sigma_v = g_{v0} \left(\Gamma_w \tilde{\omega} + \frac{d\Gamma_w}{dn_B} \tilde{\omega} n_B - \frac{d\Gamma_s}{dn_B} \tilde{\sigma} n_s \right),$$
$$\qquad (14)$$

$$\tilde{\sigma} = \Gamma_s n_s / m_s^2, \quad \tilde{\omega} = \Gamma_w n_B / m_v^2,$$

(b)

$$\Sigma_s = \tilde{\sigma} \left(\Gamma_s + \frac{d\Gamma_s}{dn_s} n_s \right), \; \Sigma_v = g_{v0} \, \tilde{\omega} \left(\Gamma_w + \frac{d\Gamma_w}{dn_B} n_B \right),$$
$$\qquad (15)$$

$\tilde{\sigma}$ and $\tilde{\omega}$ have the same expressions as in (a),

(c)

$$\Sigma_s^{AB} = \Sigma_s^{\text{isos}} \delta_{AB} + \Sigma_s^{\text{isov}\,AB},$$
$$\Sigma_v^{AB} = g_{v0} \left(\Sigma_v^{\text{isos}} \delta_{AB} + \Sigma_v^{\text{isov}\,AB} \right),$$
$$\Sigma_s^{\text{isos}} = \Gamma_s \tilde{\sigma}, \quad \Sigma_s^{\text{isov}\,AB} = \Gamma_f^{3\,AB} \tilde{\phi},$$
$$\Sigma_v^{\text{isos}} = \Gamma_w \tilde{\omega}, \quad \Sigma_v^{\text{isov}\,AB} = -\Gamma_r^{3\,AB} \tilde{\rho}, \qquad (16)$$
$$m_s^2 \tilde{\sigma} = \frac{d\Sigma_s^{\text{isos}}}{d\tilde{\sigma}} n_s, \quad m_w^2 \tilde{\omega} = \frac{d\Sigma_v^{\text{isos}}}{d\tilde{\omega}} n_B,$$
$$m_f^2 \tilde{\phi} = \left\langle \bar{\Psi} \frac{d\Sigma_s^{\text{isov}}}{d\tilde{\phi}} \Psi \right\rangle - \left\langle \bar{\Psi} \frac{d\Sigma_v^{\text{isov}}}{d\tilde{\phi}} \gamma_0 \Psi \right\rangle,$$
$$m_r^2 \tilde{\rho} = \left\langle \bar{\Psi} \frac{d\Sigma_v^{\text{isov}}}{d\tilde{\rho}} \gamma_0 \Psi \right\rangle.$$

To obtain the equations listed above, we have used the Wick theorem and the Hartree approximation; therefore, contractions of fields belonging to different full contracted terms (both in Lorentz and isospin indices) have been neglected. This approach has let us extract the vertices Γ and its derivatives from the expectation values and express the mean value of products of more than two fermion fields as product of baryonic densities and currents. Finally, we have adopted the reference frame of static matter; therefore, we have obtained $\langle j_\mu \rangle = n_B \, g_{\mu 0}$, $\langle j_\mu^c \rangle = (n_B^{(1)} - n_B^{(2)}) \, g_{\mu 0} \delta_{3c}$, with $n_B^A = \langle \bar{\psi}_A \gamma_0 \psi_A \rangle$ the number of neutrons or protons per unit volume, for $A = 2, 1$, respectively, and $n_B = n_B^{(1)} + n_B^{(2)}$ the baryonic number density. Furthermore we have introduced the simplifying notation $n_s^{(A)} = \langle \bar{\psi}_A \psi_A \rangle$, $n_s = \langle \bar{\Psi} \Psi \rangle$, $\Gamma = \langle \Gamma \rangle$, $s_1 = n_B$, $s_2 = n_s$, $s_3 = | \, n_B^{(1)} - n_B^{(2)} \, |$, $s_4 = | \, n_s^{(1)} - n_s^{(2)} \, |$, $m_1 = \tilde{\omega}$, $m_2 = \tilde{\sigma}$, $m_3 = \tilde{\rho}$, and $m_4 = \tilde{\phi}$.

Cases (a) and (b) yield meson equations that resemble those of the Walecka model [9] and nucleon self-energies with the *rearrangement* contributions added. In (c) the self-energies have the same structure as in QHD-I, but the source term of the meson equations are modified. Furthermore, it must be noted that $\langle \bar{\Psi} \tau_c \Psi \rangle = 0$ for $c = 1, 2$ as isospin is a conserved charge. To give explicit expressions for the corresponding vertices, we follow the parametrization of [4]

$$\Sigma_k^{AA\,(in)} = \frac{\alpha_k + I_3^A \beta_k t}{\lambda + n_0/n_B + I_3^A \alpha t}, \quad k = s, v, \qquad (17)$$

with $I_3^A = 1(-1)$, for protons (neutrons), $n_0 = 0.17 \, \text{fm}^{-3}$, $t = (n_B^{(2)} - n_B^{(1)})/n_B$, the remaining coefficients can be expressed in terms of the quantities used in Ref. [4] as $\lambda = C_v^q v_N + C_g^q g_N + C_{u1}^q + C_\omega^q A_{4q}^{q0}$, $\alpha = C_{u2}^q + C_\omega^q A_{4q}^{q1}$, $\alpha_s = M\lambda - C_k^I \kappa_N - C_\omega^I A_{4q}^{I0}$, $\beta_s = M\alpha - (C_\zeta^I \zeta_N + C_\omega^I A_{4q}^{I1})$, $\alpha_v = -(C_v^p v_N + M C_{u1}^p + M C_\omega^p A_{4q}^{p0})$, $\beta_v = -(C_{v-}^p v_N^- + M C_{u2}^p + M C_\omega^p A_{4q}^{p0})$, which were obtained in Ref. [4], by averaging over the Borel mass. For the sake of completeness we give here the numerical values $v_N = 3$, $v_N^- = 1$, $g_N = -8M/9$, $\kappa_N = 8$, $\zeta_N = 0.54$, $C_\kappa^I = -0.042 \, \text{GeV}$; $C_\zeta^I = -0.042 \, \text{GeV}$; $C_g^q = 0.011/\text{GeV}$; $C_{v-}^p = -0.068 \, \text{GeV}$; $C_\omega^k = -0.067, -0.095, -0.070 \, \text{GeV}$, $A_{4q}^{0k} = 1.90, -0.57, -0.11$, and $A_{4q}^{1k} = -0.92, 0.09, -0.21$ for $k = I$, p and q respectively; $C_v^k = -0.062, -0.090$, $C_{u1}^k = -0.074, 0.094$, and $C_{u2}^k = 0.008, -0.02$ for $k = q$ and p respectively. From Eq. (17), we can extract isoscalar and isovector contributions, i.e., we consider the splitting $\Sigma_k^{AA\,(in)} = \Sigma_k^{\text{isos}\,(in)} + \Sigma_{k\,A}^{\text{isov}\,(in)}$, with

$$\Sigma_k^{\text{isos}\,(in)} = \frac{\alpha_k n_B}{n_0 + \lambda n_B},$$
$$\Sigma_{k\,A}^{\text{isov}(in)} = I_3^A t \frac{\beta_k - \alpha_k' \alpha n_B}{\lambda + n_0/n_B + I_3^A \alpha t}, \qquad (18)$$

with $\alpha_k' = \alpha_k/n_0 + \lambda n_B$.

A choice of the isovector interaction in Eq. (2), that is coherent with these results is

$$\mathcal{L}_{\text{iso}} = \bar{\Psi} \tau^c \frac{G_r \, \rho_c + G_f \phi_c}{1 + g \, \tau_a \phi^a} \Psi, \qquad (19)$$

where G_r is assumed to depend only on m_3, whereas G_f and g are considered functions of only m_4. The following vertices are deduced from it:

$$\Gamma_r^c = \frac{G_r \tau^c (1 - g\tau_a \phi^a)}{1 - g^2 \phi^2}, \quad \Gamma_f^c = \frac{G_f \tau^c (1 - g\tau_a \phi^a)}{1 - g^2 \phi^2}. \quad (20)$$

In the MFA, they give rise to the following contributions to the nucleon self-energies

$$\Sigma_v^{\text{isov }AB} = -\delta_{AB} \frac{I_3^A G_r \tilde{\rho}}{1 + I_3^A g\tilde{\phi}}, \quad \Sigma_s^{\text{isov }AB} = \delta_{AB} \frac{I_3^A G_f \tilde{\phi}}{1 + I_3^A g\tilde{\phi}}. \quad (21)$$

The isovector meson field equations can now be written as follows

$$m_f^2 \tilde{\phi} = \sum_{A=1}^{2} \left(\frac{\partial \Sigma_s^{\text{isov }AA}}{\partial \tilde{\phi}} n_s^A - \frac{\partial \Sigma_v^{\text{isov }AA}}{\partial \tilde{\phi}} n_B^A \right), \quad (22)$$

$$m_r^2 \tilde{\rho} = \sum_{A=1}^{2} \frac{\partial \Sigma_v^{\text{isov }AA}}{\partial \tilde{\rho}} n_B^A. $$

In DDHFT [5–7], the isoscalar vertices Γ_s and Γ_w are defined by means of the relations

$$\Sigma_s^{(in)} = \Gamma_s n_s / m_s^2, \quad \Sigma_\mu^{(in)} = \Gamma_w n_\mu / m_w^2, \quad (23)$$

where $\Sigma_s^{(in)}$, $\Sigma_\mu^{(in)}$ are the self-energies obtained with one boson exchange potentials in the Dirac-Brueckner-Hartree-Fock approach for symmetric nuclear matter. It must be noted that the right-hand sides of these equations do not coincide in general with the dynamical self-energies. Consequently, Eqs. (14), (15), and (19) do not coincide unless the *re-arrangement* terms were omitted. However, in Ref. [11] the author proposed that the vertices are solutions of someone of the differential Eqs. (14)–(16). They must be solved together with the self-consistent condition for the meson fields. The explicit form of part of these solutions have been anticipated in Ref. [11], so we have summarized them below, and we have added new results to (c) concerning isospin asymmetric nuclear matter:

(a)

$$\Gamma_s = \frac{\Sigma_s^{(in)}}{\tilde{\sigma}}, $$
$$(24)$$
$$\Gamma_w^2 = 2 \left(\frac{m_w}{n} \right)^2 \int_0^{n_B} dn' \left[\Sigma_v^{(in)} + \left(\frac{n_s}{m_s} \right)^2 \Gamma_s \frac{d\Gamma_s}{dn'} \right]; $$

(b)

$$\Gamma_s^2 = 2 \left(\frac{m_s}{n_s} \right)^2 \int_0^{n_B} dn' \frac{dn_s}{dn'} \Sigma_s^{(in)}, $$
$$(25)$$
$$\Gamma_w^2 = 2 \left(\frac{m_w}{n_B} \right)^2 \int_0^{n_B} dn' \Sigma_v^{(in)}; $$

(c)

$$\Gamma_s = \Sigma_s^{\text{isos }(in)} / \tilde{\sigma}, \quad \Gamma_w = \Sigma_v^{\text{isos }(in)} / \tilde{\omega}, \quad g = \frac{\alpha t n_B}{\tilde{\phi}(n_0 + \lambda n_B)}, \quad (26)$$

$$G_f = \frac{\beta_s - \alpha_s' \alpha n_B}{n_0 + \lambda n_B} \frac{t n_B}{\tilde{\phi}}, \quad G_r = -\frac{\beta_v - \alpha_v' \alpha n_B}{n_0 + \lambda n_B} \frac{t n_B}{\tilde{\rho}}, \quad (27)$$

$$\tilde{\sigma}^2 = \frac{2}{m_s^2} \int_0^{n_B} dn' \, n_s \frac{d\Sigma_s^{\text{isos }(in)}}{dn'}, $$
$$(28)$$
$$\tilde{\omega}^2 = \frac{2}{m_w^2} \int_0^{n_B} dn' \, n' \frac{d\Sigma_v^{\text{isos }(in)}}{dn'}, $$

$$\tilde{\phi}^2 = \frac{1}{m_f^2} \sum_{A,C=1}^{2} (1 - I_3^C t) \int_0^{n_B} dn' \left[n_s^A \frac{\partial \Sigma_{s A}^{\text{isov }(in)}}{\partial n_C'} \right. $$
$$\left. - \frac{1}{2} n' (1 - I_3^A t) \frac{\partial \Sigma_{v A}^{\text{isov }(in)}}{\partial n_C'} \right], \quad (29)$$

$$\tilde{\rho}^2 = \frac{1}{2m_r^2} \sum_{A,C=1}^{2} (1 - I_3^C t)(1 - I_3^A t) $$
$$\times \int_0^{n_B} dn' n' \frac{\partial \Sigma_{v A}^{\text{isov }(in)}}{\partial n_C'}. \quad (30)$$

We have assumed that the input functions have been parametrized in terms of the partial nucleon densities n_C; furthermore, within the two last equations of (c), the isospin parameter t is held constant in the integration.

Thus, we have obtained a set of relations, that defines a hadronic field model suited to reproduce the nucleon self-energies provided by other theoretical framework. In particular, the meson-dependent vertices have been extended to deal with isospin asymmetric matter. The resulting vertices are given as functions of n_B, and eventually s_3, but they can be rewritten in terms of the meson fields or nucleon condensates.

In the next section, these results are compared with the standard DDHFT treatment, and the ability to adjust the nuclear matter phenomenology is examined.

III. RESULTS AND DISCUSSION

A well-known feature of isospin symmetric nuclear matter is that its energy per particle has a minimum at a baryonic density of $n_0 = 0.16 \, \text{fm}^{-3}$. This property gives rise to bound states at zero temperature, and it is the minimum requirement that a model of nuclear matter should satisfy. Starting with Eq. (2), we have evaluated the energy-momentum tensor $T^{\mu\nu}$ by the canonical procedure, and the energy per unit volume in the MFA is obtained by taking the in-medium expectation value of T^{00}

$$E_{\text{MFA}} = \int_0^{p_F} \frac{d^3 p}{(2\pi)^3} \sqrt{p^2 + M^{*2}} + \Gamma_w n_B \tilde{\omega} $$
$$+ n_s (\Sigma_s^{\text{isos}} - \Gamma_s \tilde{\sigma}) + \frac{1}{2} (m_s^2 \tilde{\sigma}^2 - m_w^2 \tilde{\omega}^2), \quad (31)$$

where we have introduced the Fermi momentum p_F, related to the baryonic density by $n_B = 2p_F^3/(3\pi^2)$, and the effective nucleon mass $M^* = M - \Sigma_s$. The mean value of the isovector meson fields becomes zero for symmetric nuclear matter.

Finally, the binding energy is defined as $E_B = E_{\text{MFA}}/n_B - M$, which should have a minimum value $E_B \simeq -16$ MeV at the normal density n_0 to satisfy the nuclear matter phenomenology. Using the thermodynamical relation $P = \mu n_B - E_{\text{MFA}}$ we have obtained the pressure for the nuclear matter; the chemical potential is given by $\mu = E_F + \Sigma_v^{\text{isos}}$ with $E_F = \sqrt{p_F^2 + M^{*2}}$.

First, we have examined the effects of introducing the effective vertices by means of the algebraic Eqs. (23) or by solving a differential equation of the types shown in Eqs. (14)–(16). It must be noted that the first option has the property of reproducing the energy density of the original Dirac-Brueckner calculations, as long as the parametrization of the vertices in terms of only the baryon number density is chosen. The alternative procedure proposed in Ref. [11] aims to make a connection between the hadronic vertices and another theoretical framework by imposing the equality of the input functions and the nucleon self-energies evaluated with the hadronic model in the Hartree approach.

For the purpose stated, we have chosen as input the results of Ref. [8]. In this work, an ansatz for the vertices is proposed that fits several specific Dirac-Brueckner outcomes, but it avoids the unphysical behavior they exhibit in the zero density limit. The ansatze for the couplings Γ_s^{TW} and Γ_w^{TW} are rational functions of the relative baryonic density n_B/n_0. The corresponding self-energies are obtained as $\Sigma_s^{(in)} = \Gamma_s^{\text{TW}}\tilde{\sigma}$, $\Sigma_v^{(in)} = \Gamma_w^{\text{TW}}\tilde{\omega}$, with the meson mean-field values given by equations similar to those of Eq. (14). For details, see Ref. [8].

In Fig. 1 we show the binding energy and pressure evaluated within the standard DDHFT treatment of Ref. [8]. Given the functions $\Sigma_s^{(in)}$, $\Sigma_v^{(in)}$ as above, we can also use them to deduce the vertices Γ_s, Γ_w, which reproduce these self-energies within the approach (a); i.e., solving Eqs. (14). The corresponding equation of state is shown in the same figure. We have examined densities up to 4 times n_0, a range that may be reached inside neutron stars. It can be seen that similar results for the pressure are obtained for densities below $1.25n_0$, but the binding energy shows appreciable differences. These results are qualitatively comparable; however, for high densities the standard DDHFT treatment yields slightly less growth for both E_B and P. These differences could be significant for those phenomena dominated by the regime of extreme densities, such as the structure of neutron stars.

Second, we have examined the effect of multiple representations. When a set of functions Σ_s, Σ_μ, depending on the macroscopic variables of nuclear matter is given, there is an indefinite number of models, such as that of Eq. (2), capable of reproducing them within MFA. Some of these possibilities have been listed as (a)–(c) in the previous section. The formal aspects have been summarized in Eqs. (14)–(16); now we are going to focus on some thermodynamical observables of symmetric nuclear matter.
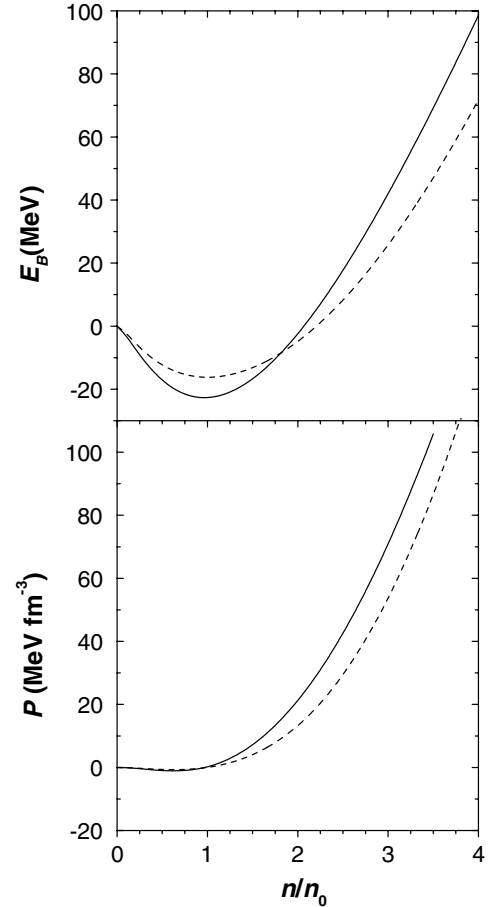

FIG. 1. The binding energy and the pressure for symmetric nuclear matter at zero temperature, evaluated in the MFA using the standard DDHFT treatment (dashed lines) and within approach (a) (solid lines).

To avoid biased conclusions, we have considered two inputs of diverse sources. In addition to the results of Ref. [8], based on one-boson exchange potentials, we have included the QCD sum-rules calculations of Ref. [4]. We have evaluated the binding energy and the pressure, for each of these inputs under the three assumptions (a)–(c). We have found that despite the different parametrizations used for a given input, the results are practically undistinguishable in both cases. This feature, for the calculations using the inputs obtained from Ref. [4], is shown in Fig. 2. As it can be seen that the three curves are nearly coincident. The range of densities has been restricted to the region of validity of the QCD sum-rules computations. The binding energy is monotonically decreasing; it seems to have a minimum near $n \simeq 2n_0$, where the effective nucleon mass tends to zero. This description does not adjust to the nuclear matter phenomenology; however, we keep Ref. [4] in consideration as it offers a physically meaningful input. It must be noted that the result (c) does not coincide with the preliminary result given in Ref. [11], as the ω-meson contribution to the energy was not properly taken into consideration there.

A similar conclusion is obtained by using the self-energies extracted from Ref. [8], because the curves
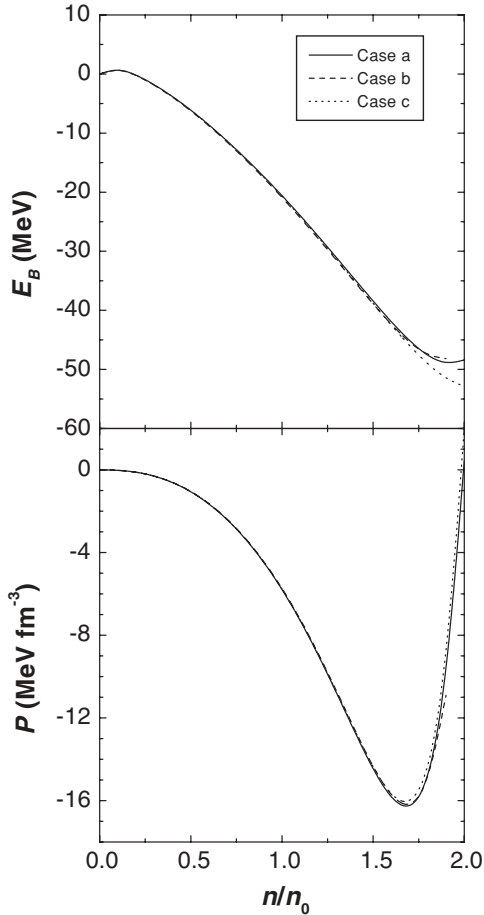
FIG. 2. The binding energy and the pressure obtained by using the results of Ref. [4] within the approaches (a)–(c).The line convention for both cases is indicated in the upper panel.
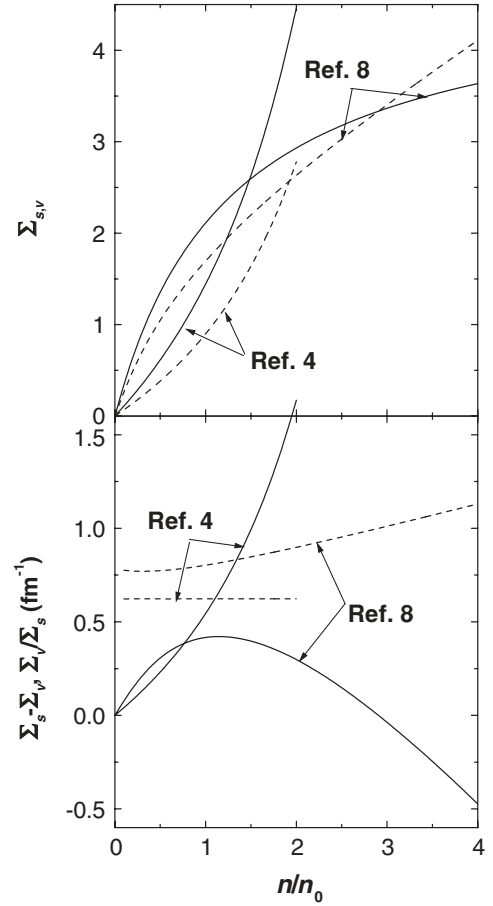

FIG. 3. The nucleon self-energies for symmetric nuclear matter, provided by Refs. [8] and [4]. (Upper panel) The magnitudes of $\Sigma_s^{(in)}$ (solid lines) and $\Sigma_v^{(in)}$ (dashed lines); (lower panel) the difference (solid lines) and the ratio (dashed lines) between the scalar and vector components.

corresponding to the instances (b) and (c) (not shown in the figure) follow the solid curves of Fig. 1 closely, in the full range $0 < n < 4\,n_0$.

The different behavior between the inputs obtained from Refs. [4] and [8] for the energy per particle can be justified by examination of Fig. 3. In the upper panel, the self-energies as functions of the density show a monotonous increase in both cases. However, the rate of growth of Σ_s is lower than that for Σ_v for densities $n \geqslant n_0$ in the parametrization of Ref. [8]. On the contrary, the QCD sum-rules outputs maintain a faster increase of the scalar as compared to the vector self-energy over the domain of densities. This behavior is emphasized in the bottom panel, where the difference $\Sigma_s - \Sigma_v$ steadily increases in one case but exhibits an extremum in the other one. Furthermore, a constant quotient Σ_v/Σ_s is obtained for the QCD sum-rules input, but it increases slowly for the other instance. The density dependence of the vertices, which were obtained by using the input of Ref. [8] under the three approaches (a)–(c) is presented in Fig. 4. It must be noted that the expressions for $\Gamma_{s,w}$ become singular at zero density; nevertheless, they have finite limits: $\Gamma_s^2 \rightarrow m_s^2 d\Sigma_s^{(in)}/dn$, $\Gamma_w^2 \rightarrow m_w^2 d\Sigma_v^{(in)}(0)/dn$, for all cases under consideration.

A common feature of the vertices is a strong decrease up to $n \leqslant 2n_0$. This decrease becomes more moderate for higher density values. The cases (b) and (c) yield very similar results for both Γ_s and Γ_w, whereas the noticeable differences respect to the case (a) may lead to qualitatively distinct descriptions for subsequent applications. All these results for the vertices $\Gamma_k(z)$ can be summarized by an expression in terms of its natural variable z, $\Gamma_k = (z + a_k)/\big[b_k + c_k(z + a) + d_k(z + a)^2\big]$, with $k = s, w$; the numerical coefficients are shown in Table I.

Another insight into the basic phenomenology of nuclear matter can be given by the Landau parameters. They can be evaluated as the Legendre projections of the second derivative of E_{MFA} with respect to the baryonic density; for a discussion the reader should see Ref. [14]. These parameters are very useful in regard to collective phenomena of the dense nuclear environment, as, for instance, phase transitions, the giant monopolar and quadrupolar modes, or the sound velocity [15]. To keep track of the momentum dependence, we assume a nonzero spatial component of the self-energy $\vec{\Sigma}_v$, the baryonic current $\vec{j}$, and the omega meson $\vec{\omega}$, taking the zero limit of these quantities at the end of the calculations. So, for instance, we write $E_p = \sqrt{(\vec{p} - \vec{\Sigma})^2 + M^{*2}}$ into the integral of Eq. (31).
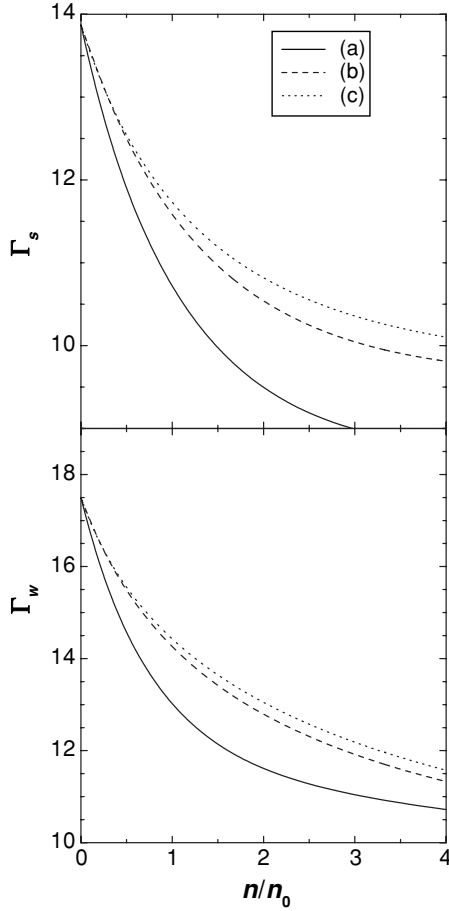
FIG. 4. The effective nucleon-meson vertices as functions of the baryonic density for cases (a)–(c). The line convention for both cases is indicated in the upper panel.

Denoting with n_k the occupation number of nucleon states with a well-defined momentum $\vec{p}_k$, we define

$$
\begin{aligned}
f_{kl} &= \frac{\partial^2 E_{\text{MFA}}}{\partial n_k \partial n_l} \\
&= -\frac{M^*}{E_i} \frac{\partial \Sigma_s}{\partial n_l} + \frac{\partial \Sigma_v}{\partial n_l} - \frac{\vec{p}_k}{E_k} \cdot \frac{\partial \vec{\Sigma}_v}{\partial n_l} - \frac{\partial \vec{\Sigma}_v}{\partial n_k} \\
&\quad \cdot \left(\frac{\partial \vec{j}}{\partial n_l} - \frac{n_s}{M^*} \frac{\partial \vec{\Sigma}_v}{\partial n_l} \right) + m_w^2 \frac{\partial \vec{\omega}}{\partial n_k} \cdot \frac{\partial \vec{\omega}}{\partial n_l};
\end{aligned}
\tag{32}
$$

in the second equality, the limit of isotropic nuclear matter has been taken. The derivative of the baryonic current can be evaluated in the MFA as follows:

$$
\frac{\partial \vec{j}}{\partial n_i} = \frac{\vec{p}_i}{E_i} - H \frac{\partial \vec{\Sigma}_v}{\partial n_i}, \quad H = \frac{1}{6\pi^3} \int_0^{p_f} d^3 p \, \frac{2p^2 + 3M^{*2}}{(p^2 + M^{*2})^{3/2}}.
\tag{33}
$$

The remaining derivatives are

$$
\frac{\partial \vec{\omega}}{\partial n_i} = \frac{\tilde{\omega}}{n} \frac{\partial \vec{j}}{\partial n_i}, \quad \frac{\partial \vec{\Sigma}_v}{\partial n_i} = \frac{\vec{p}_i}{E_i} \frac{\Sigma_v}{n + H \Sigma_v},
\tag{34}
$$

the explicit formulas depends on the approach used [(a)–(c)].

The Landau parameters f_k are defined by means of the projections

$$
f_m = \frac{2m+1}{2} \int_{-1}^{1} f_{kl} P_m(\nu) d\nu,
\tag{35}
$$

with ν the cosine of the angle between $\vec{p}_k$ and $\vec{p}_l$, and P_m the Legendre polynomial of order m. At the end of the calculations, the replacement $|\vec{p}_k|, |\vec{p}_l| \to p_F$ is made. By this procedure, we have obtained the Landau parameters of zero and first orders

$$
f_0 = -\frac{M^*}{E_F} \frac{d\Sigma_s^{(inp)}}{dn} + \frac{d\Sigma_v^{(inp)}}{dn},
\tag{36}
$$

$$
\begin{aligned}
f_1 &= \left(\frac{p_F/E_F}{n + H \Sigma_v^{(inp)}} \right)^2 \\
&\quad \times \left[m_w^2 \tilde{\omega}^2 - 2n \Sigma_v^{(inp)} + \left(\frac{n_s}{M^*} - H \right) \Sigma_v^{(inp)\,2} \right].
\end{aligned}
\tag{37}
$$

It is custumary to normalize the Landau parameters with the density of states at the Fermi surface $\varepsilon_F = 2p_F E_F/\pi^2$, so that $F_k = \varepsilon_F f_k$.

For a given model of self-energies, the result for f_0 does not depend on the field parametrization of the vertices. The parameter f_1 instead depends on $\tilde{\omega}$, which certainly differs for each of the instances (a)–(c). In Fig. 5 the density dependence of both Landau parameters is shown, and significant differences for f_1 are found for densities above $0.25n_0$.

Consequently, all physical magnitudes depending solely on f_0, such as the nuclear compressibility $K = 3p_F^2(1 + F_0)/E_F$, do not distinguish among the field parametrization of the vertices. The same feature is shared by the giant monopole mode energy $E_M = \alpha_0/A^{1/3}$, with $\alpha_0 \simeq 1.076\sqrt{K/\mu}$, and the first sound velocity $v_1 = p_F\sqrt{(1 + F_0)/(3\mu E_F)}$. However, the excitation energy of the quadrupole state is given by $E_Q = \alpha_2/A^{1/3}$, with $\alpha_2 = p_F\sqrt{2}/(1.2\mu\sqrt{1 + F_1/3})$; therefore, it is sensitive to the approach used. We have obtained in our calculations $K \simeq 440$ MeV, $\alpha_0 \simeq 145$ MeV, and $\alpha_2 \simeq 77$ MeV at the normal

TABLE I. Numerical values of the fitting coefficients for the density dependence of the vertices, obtained in the approaches (a)–(c) using the self-energies deduced from Ref. [8].

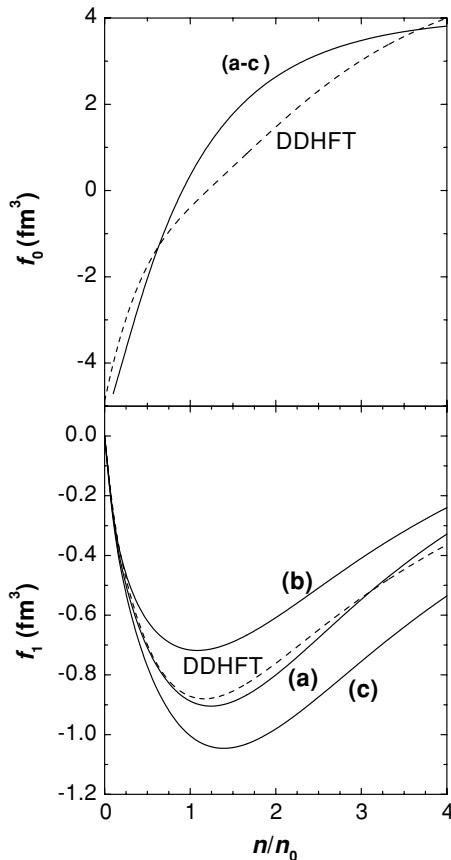| Case	a_s	b_s	c_s	d_s	a_w	b_w	c_w	d_w	z_s	z_w
(a)	0.805	−0.170	0.350	−0.082	0.386	−0.032	0.148	−0.024	s_1	s_1
(b)	1.264	−0.232	0.294	−0.031	0.413	−0.018	0.096	0.009	s_2	s_1
(c)	0.059	0.000	0.066	0.078	1.178	−0.217	0.285	−0.037	m_2	m_1

FIG. 5. The Landau parameters of zero (top) and first (bottom) order in terms of the baryonic density under the three cases [(a)–(c)] and the standard DDHFT treatment.

FIG. 6. The low lying collective longitudinal modes in terms of the baryonic density under the three cases (a)–(c) and the standard DDHFT treatment.

density, which must be compared with the empirical values $230 \, \text{MeV} < K < 270 \, \text{MeV}$, $\alpha_0 = 80 \, \text{MeV}$, and $\alpha_2 = 63 \, \text{MeV}$.

Another interesting phenomenological property that can be related to the Landau parameters are the zero-sound modes. These are longitudinal collective modes propagating in nuclear matter at zero temperature, whose dispersion relation can be found as the zeros of the longitudinal dielectric function

$$\varepsilon_L = 1 + \left(F_0 + \frac{F_1 \, Q^2}{1 + F_1/3} \right) \Phi(Q), \qquad (38)$$

with $Q = p_0 E_F / (|\vec{p}| p_F)$ and Φ the Lindhard function. Collective modes have been studied in detail within relativistic field models, the reader should see, for instance Refs. [14–18]. Low-lying collective modes can be classified as instability modes, in the low-density realm, and zero-sound modes, with a characteristic linear dispersion relation $p_0 \propto |\vec{p}|$. In Fig. 6, the dispersion relation in terms of the baryonic density is shown for the standard DDHFT treatment and for the approaches (a)–(c) within the self-energy parametrization of Ref. [8]. These results are appropriate for the realm $|\vec{p}| \rightarrow 0$ while maintaining the linear dispersion relation. The instability and zero-sound modes are clearly distinguishable, the first ones are closely related to the equation of state and, therefore, all the corresponding curves practically coincide. The zero-sound mode yields very different behaviors; the extremum values for
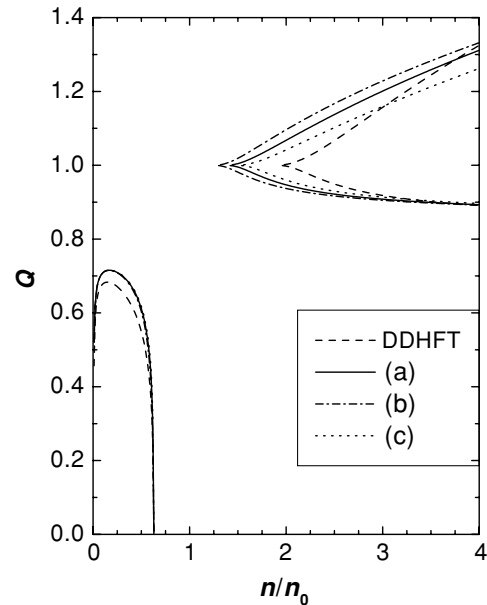
its threshold are obtained within the approaches (b) and the standard DDHFT treatment. We have obtained $n/n_0 = 1.25$ and 2, respectively. In all cases, we have obtained two-fold zero-sound, and, taking into account that $\Phi(Q)$ has a nonzero imaginary part for $Q < 1$, only the upper mode is undamped.

IV. SUMMARY AND CONCLUSIONS

In this work we have examined two definitions of the vertices of a hadronic field model in terms of the self-energies provided by another theoretical framework. The first one is the standard DDHFT treatment, which uses Eqs. (23) to define the meson-nucleon vertices. In these equations $\Sigma^{(in)}$ denotes the nucleon self-energies taken as input, which are evaluated in the Dirac-Brueckner approach with one-meson exchange potentials. Although vector and scalar dependencies have been stated [7], most practical applications have used only the first one, similar to our case (a). This particular choice has the property of reproducing the equation of state of the source calculations; on the contrary, the model self-energies differ from the inputs $\Sigma^{(in)}$. An alternative definition was proposed in Ref. [11]; it consists of equating both the input self-energy and the one evaluated within the hadronic model with vertices depending on scalar combinations of hadronic fields. This procedure ensures a coherent overlap of the effective hadronic field model and a more *fundamental* theoretical description, at least in the baryon sector. Three different parametrizations of the vertices [cases (a)–(c)] and two theoretical sources (the QCD sum rules of Ref. [4] and the Dirac-Brueckner approach of Ref. [8]) have been examined within this scheme.

Thermodynamical aspects of symmetric nuclear matter evaluated according to the prescriptions (a)–(c) are undistinguishable within the MFA. On the contrary, they differ

noticeably from the standard DDHFT results. Although the almost perfect coincidence within the (a)–(c) approaches for the energy and pressure, the obtained vertices present significant deviations in the medium- to high-density realm. The results for Γ_s, Γ_w are similar in (b) and (c), as they use parametrizations in terms of variables strongly related in the MFA. Taking the nucleon self-energies proposed in Ref. [4], we have presented formal expressions for the vertices of a hadronic field model for both isoscalar and isovector channels. We have given fittings for all the vertices in terms of its proper variables.

In reference to the theoretical source for the inputs, the parametrization given in Ref. [8] yields observables in agreement with the nuclear matter phenomenology, as expected. On the contrary, the QCD sum rules do not provide an acceptable description, at least in its present status. This assertion contrasts with the preliminary results of Ref. [11], which does not take properly the vector meson contribution to the energy density.

We have also considered in detail the Landau parameters for symmetric nuclear matter, under the four assumptions and the parametrization of Ref. [8]. The hadronic model yields two nonzero Landau parameters F_0 and F_1; the first one has a common behavior within approaches (a)–(c), whereas the second one strongly depends on the structure of the vertices. Therefore, nuclear observables depending on only F_0, such as isothermal compressibility, first-sound velocity, and the giant monopole energy, give almost coincident values. Those quantities depending on F_1 may discriminate among the different approaches; for instance, the zero-sound modes exhibit very different threshold density, according to the choice made.

To sum up, we have compared several formal schemes of merging external physical information into hadronic field models. For this purpose we have introduced interaction vertices Γ_s and Γ_w, which are functionals of the hadronic fields, and we have determined them by use of the standard DDHFT procedure or by requiring the reproduction of the self-energies used as input. It was found that different field parametrization of the vertices provide a coherent description of the nuclear matter equation of state. However, physical quantities can be found, that can distinguish among the different approaches.

QCD sum-rules calculations for the nucleon self-energy do not meet the requirements of the procedure, however, further refinements could improve its performance.

[1] M. A. Shifman, A. I. Vainshtein, and V. I. Zakharov, Nucl. Phys. **B147**, 385 (1979).

[2] B. L. Ioffe, Nucl. Phys. **B188**, 317 (1981).

[3] E. G. Drukarev and E. M. Levin, Nucl. Phys. **A511**, 679 (1990); **A532**, 695 (1991); Prog. Part. Nucl. Phys. **27**, 77 (1991); E. G. Drukarev, M. G. Ryskin, V. A. Sadovnikova, Th. Gutsche, and A. Faessler, Phys. Rev. C **69**, 065210 (2004).

[4] E. G. Drukarev, M. G. Ryskin, and V. A. Sadovnikova, Phys. Rev. C **70**, 065206 (2004).

[5] R. Brockmann and H. Toki, Phys. Rev. Lett. **68**, 3408 (1992).

[6] S. Haddad and M. K. Weigel, Phys. Rev. C **48**, 2740 (1993).

[7] H. Lenske and C. Fuchs, Phys. Lett. **B345**, 355 (1995).

[8] S. Typel and H. H. Wolter, Nucl. Phys. **A656**, 331 (1999).

[9] B. D. Serot and J. D. Walecka, Adv. Nucl. Phys. **16**, 1 (1986); B. D. Serot, Rep. Prog. Phys. **55**, 1855 (1992).

[10] S. Typel, Phys. Rev. C **71**, 064301 (2005).

[11] R. Aguirre, Phys. Lett. **B611**, 248 (2005).

[12] G. E. Brown and M. Rho, Phys. Rev. Lett. **66**, 2720 (1991).

[13] G. Q. Li, C. M. Ko, and G. E. Brown, Phys. Rev. Lett. **75**, 4007 (1995); Nucl. Phys. **A606**, 568 (1996); G. Q. Li, C. M. Ko, G. E. Brown, and H. Sorge, *ibid.* **A611**, 539 (1996).

[14] T. Matsui, Nucl. Phys. **A370**, 365 (1981).

[15] S. Nishizaki, H. Kurasawa, and T. Suzuki, Nucl. Phys. **A462**, 687 (1987).

[16] K. Lim, and C. J. Horowitz, Nucl. Phys. **A501**, 729 (1989).

[17] J. C. Caillon, P. Gabinski, and J. Labarsouque, Nucl. Phys. **A696**, 623 (2001); J. Phys. G **29**, 2291 (2003).

[18] V. Greco, M. Colonna, M. Di Toro, and F. Matera, Phys. Rev. C **67**, 015203 (2003).